

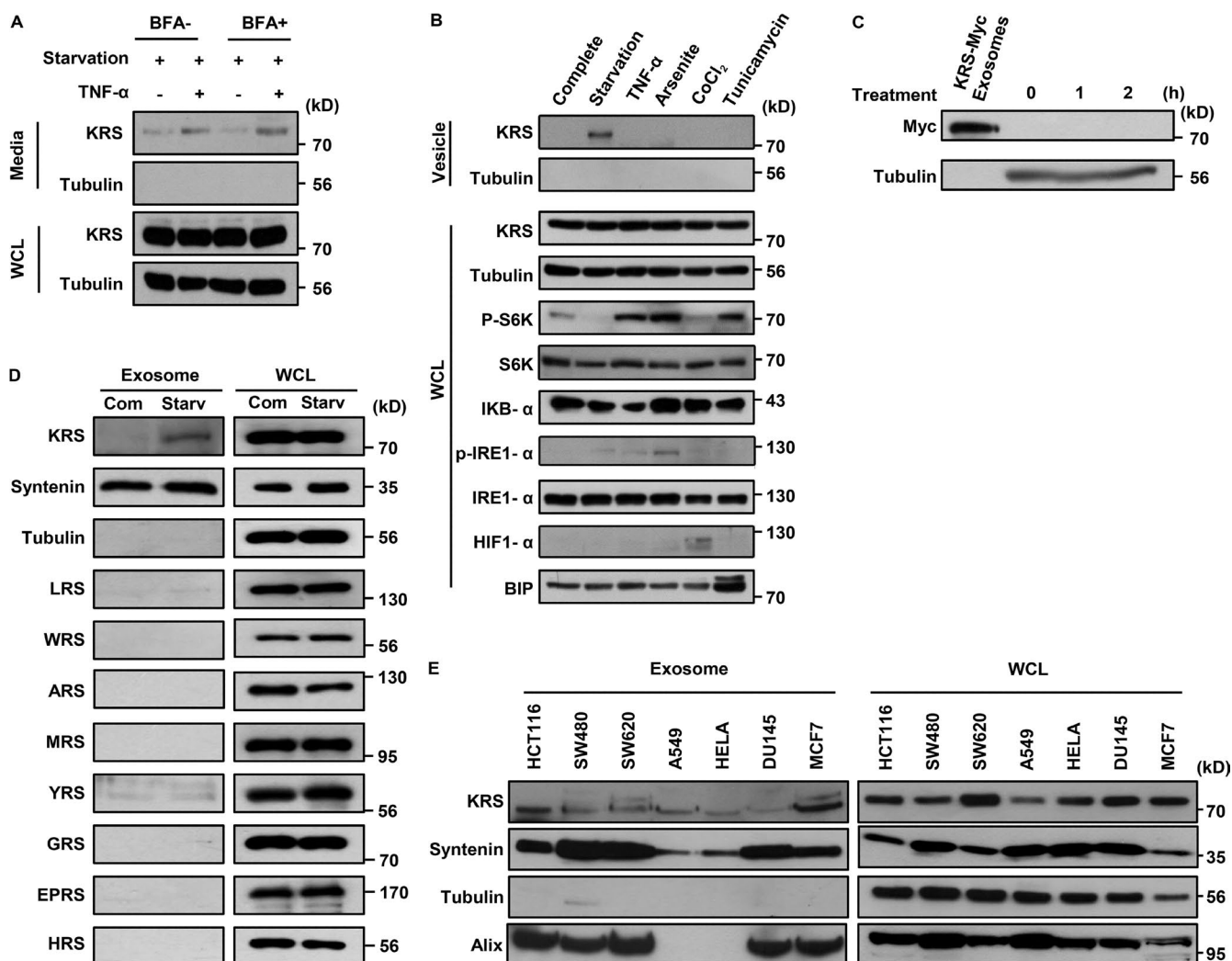
Kim et al., <https://doi.org/10.1083/jcb.201605118>

Figure S1. **Determination of KRS secretion conditions and exosome secretion of ARSs in different cell lines.** (A) HCT116 cells were pretreated with BFA (2.5 µg/ml) and incubated in starvation condition with or without TNF-α (10 ng/ml). The secretion of KRS from HCT116 cells was determined by immunoblotting of KRS in harvested media after 12 h of starvation. (B) HCT116 cells were subjected to starvation and to treatment with TNF-α (10 ng/ml), sodium arsenite (12.5 µM), CoCl<sub>2</sub> (100 µM), and tunicamycin (2 µg/ml) in complete media to induce inflammatory, reactive oxygen species (Barchowsky et al., 1999; Ruiz-Ramos et al., 2009), hypoxic (Piret et al., 2002), and ER stresses, respectively. Extracellular vesicles secreted into the media were obtained by ultracentrifugation as described in the Exosome isolation section of Materials and Methods, and the presence of KRS was determined by immunoblotting of proteins within the vesicles. BIP, binding immunoglobulin protein. (C) Exosomes were isolated from HCT116 cells transfected with KRS-Myc and incubated with macrophages. The exosome-treated macrophages were harvested at time intervals, and KRS present in macrophages was then detected by immunoblotting with anti-Myc antibody to see whether KRS-Myc in the exosomes was present as the intact form. (D) HCT116 cells were incubated in normal (complete media; com) and starvation conditions for 24 h. The culture medium was harvested and subjected to ultracentrifugation at 100,000 g to obtain a pellet. The presence of different ARSs in the isolated exosomes was detected by immunoblotting with their specific antibodies. GRS, glycyl-tRNA synthetase; HRS, histidyl-tRNA synthetase; LRS, leucyl-tRNA synthetase; MRS, methionyl-tRNA synthetase; WRS, tryptophanyl-tRNA synthetase; YRS, tyrosyl-tRNA synthetase. (E) The indicated cancer cells were incubated in starvation conditions for 24 h. The culture medium was harvested and subjected to ultracentrifugation at 100,000 g to obtain a pellet. KRS present in the isolated exosomes (10 µg total proteins) was detected by immunoblotting with anti-KRS antibody. WCL, whole-cell lysate.

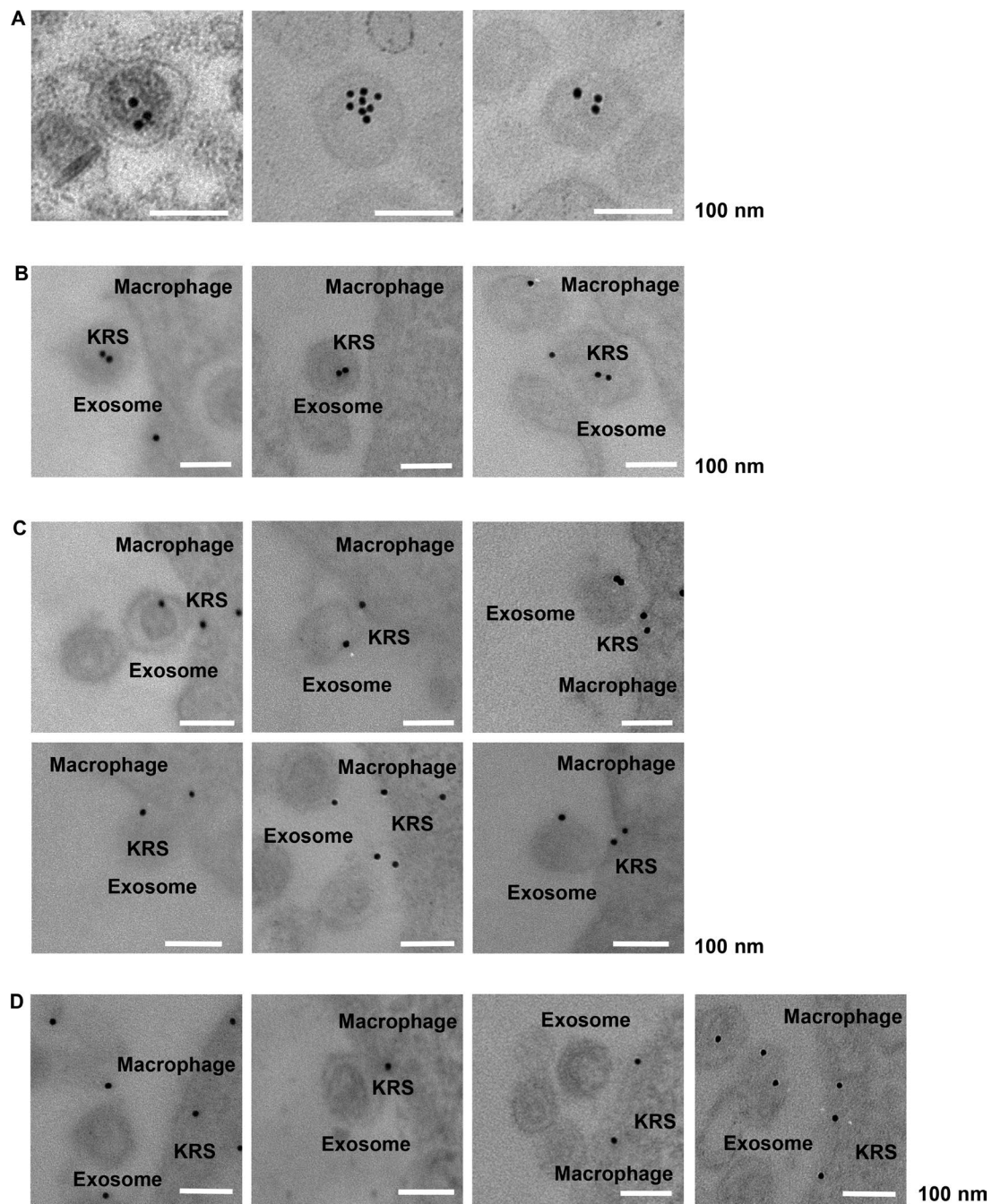
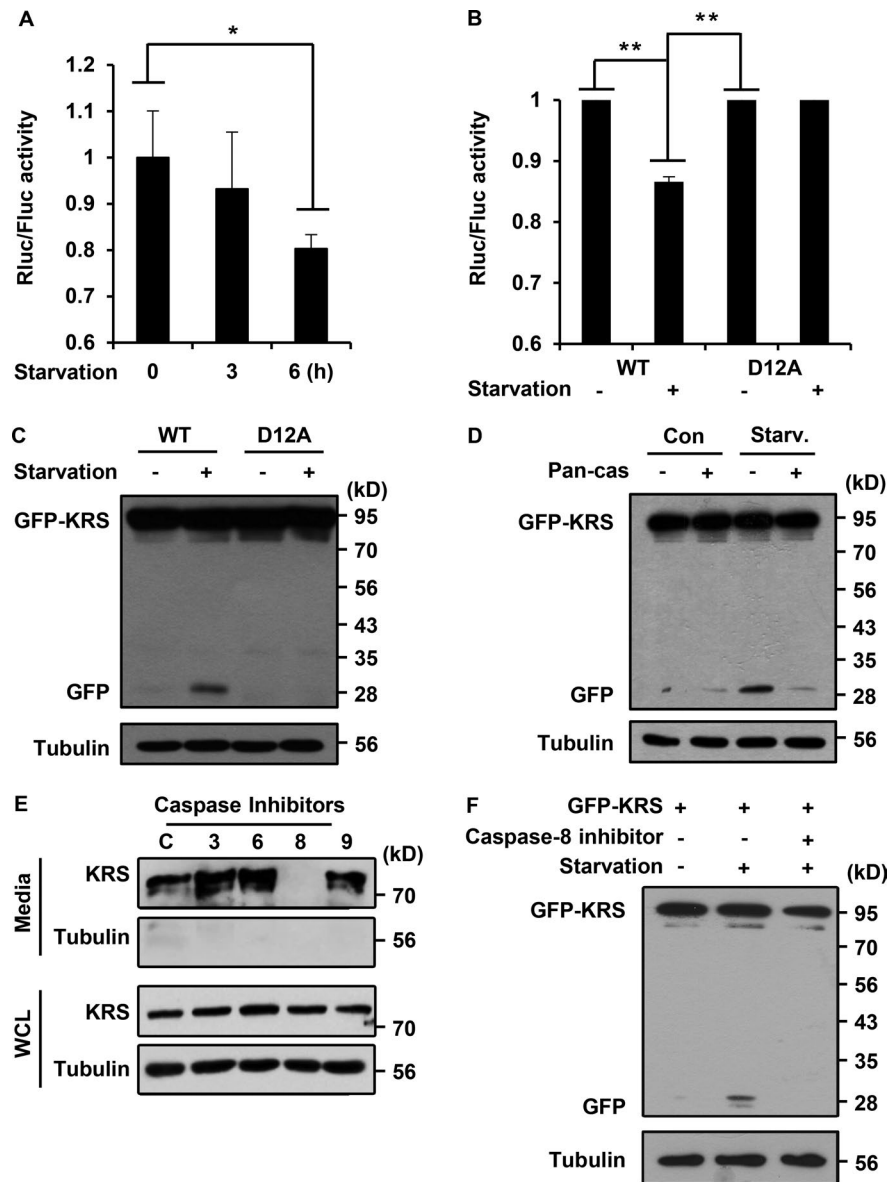


Figure S2. **Determination of KRS locations by immunogold-staining EM in the isolated exosomes and target cells.** (A and B) The location of KRS in the exosomes isolated from starved HCT116 cells (A) near the target macrophages (B). (C and D) The secreted KRS incorporation into macrophages are shown.



**Figure S3. The role of cleavage at D12 in KRS secretion and caspase-8 involvement in N-terminal cleavage of secreted KRS.** (A) To quantify the N-terminal truncation of KRS, we fused the two domains of Renilla luciferase (Rluc) to each end of KRS (N-Renilla-KRS-C-Renilla) and expressed it in HCT116 cells under starvation (Starv.) conditions. The Renilla luciferase activities relative to those of firefly luciferase (Fluc) were determined at time intervals and displayed as a bar graph. (B) Effects of starvation and D12A mutation on the N-terminal cleavage of KRS were also monitored using a Renilla luciferase assay as in A. Error bars show means  $\pm$  SD from the mean of three experiments.  $n = 3$ . \*,  $P < 0.05$ ; \*\*,  $P < 0.01$ . (C) Effect of D12A mutation on starvation-induced N-terminal cleavage of KRS was determined using GFP-KRS fusion protein expressed in HCT116 cells. (D) HCT116 cells expressing GFP-KRS were incubated in starvation medium in the absence and presence of pan-caspase (pan-cas) inhibitor for 1 h. Cleavage of KRS was monitored by immunoblotting with anti-GFP antibody. (E) The starvation-induced secretion of KRS from HCT116 cells was determined by immunoblotting of the media in the presence of specific caspase inhibitors (Z-VAD-DQMD, Z-VAD-VEID, Z-VAD-IETD, and Z-VAD-LEHD for caspase-3, -6, -8, and -9, respectively). Proteins in the media were precipitated with TCA, and KRS levels were determined by immunoblotting with anti-KRS antibody. WCL, whole-cell lysate. (F) HCT116 cells expressing GFP-KRS WT incubated in normal and starvation conditions were subjected to caspase-8 inhibitor (Z-VAD-IETD) treatment for 1 h, and the cleavage of GFP-KRS was determined by immunoblotting with anti-GFP antibody.

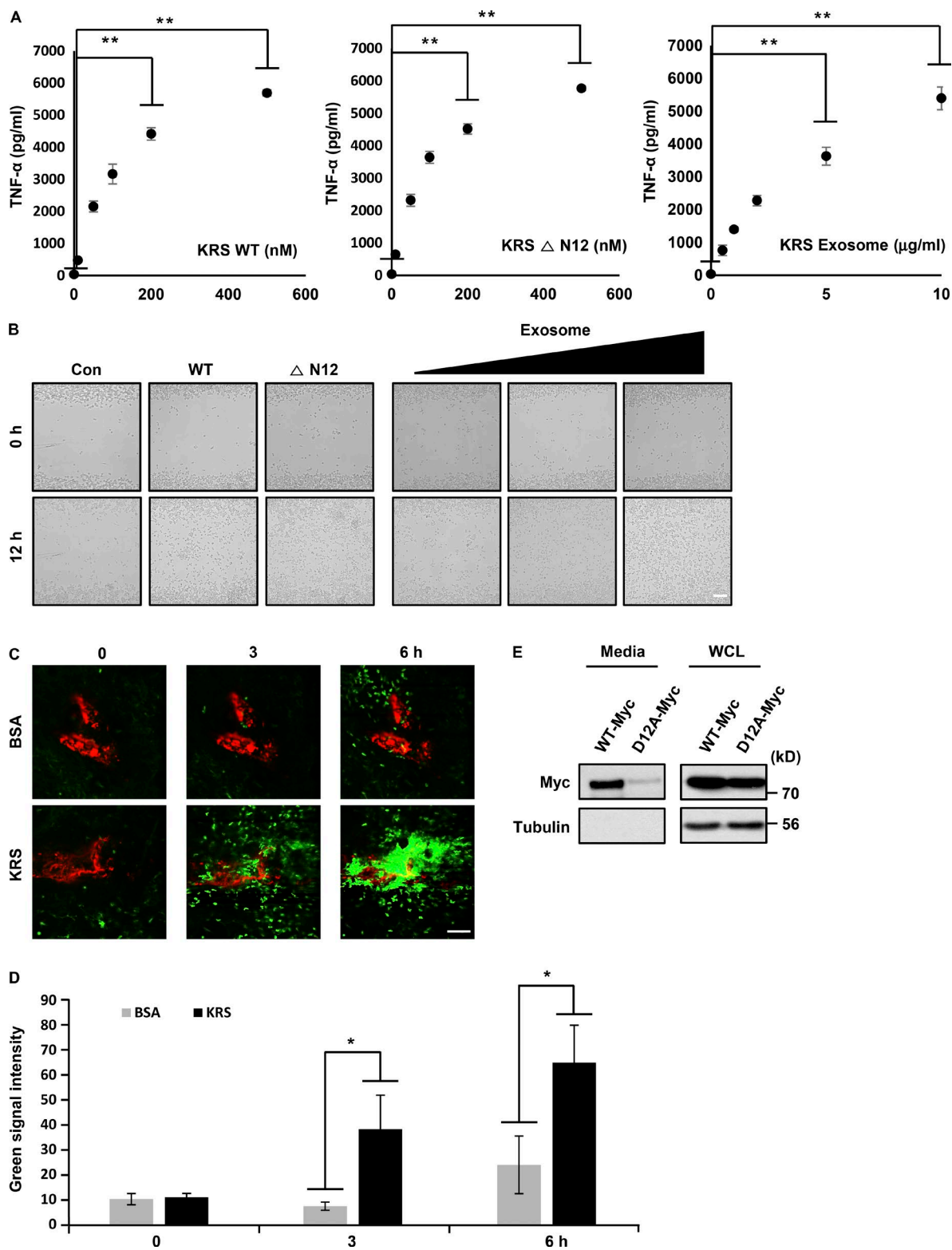


Figure S4. **Biological activities of KRS-containing exosomes.** (A) The dose-dependent effects of KRS WT, ΔN12 mutant (10, 50, 100, 200, and 500 nM), and KRS exosomes (0.5, 1, 2, 5, and 10 μg/ml) on the secretion of TNF-α from RAW264.7 cells were determined. The secretion of TNF-α was quantified using a TNF-α-specific ELISA. (B) The effects of KRS exosomes, KRS WT, and ΔN12 mutants on the migration of RAW264.7 cells were determined by a wound-healing assay (Liang et al., 2007). RAW264.7 cells were scratched and treated with KRS proteins (WT and ΔN12) and KRS exosomes. After 12-h incubation, cell migration was monitored by microscopy. (C) KRS WT and BSA were labeled with Alexa Fluor 647 and injected into mouse ear dermis (0.1 μg/μl). The recruitment of macrophages/monocytes (green) was monitored by time-lapse intravital microscopy. Bars, 100 μm. (D) These experiments were repeated three times, and the data are represented in bar graphs. Green fluorescence signal was measured by ImageJ. Error bars show means ± SD from the mean of three experiments.  $n = 3$ . \*,  $P < 0.05$ ; \*\*,  $P < 0.01$ . (E) The secretion of KRS from B16F10 cells expressing KRS-Myc (WT and D12A mutant) was determined by immunoblotting of the harvested media.

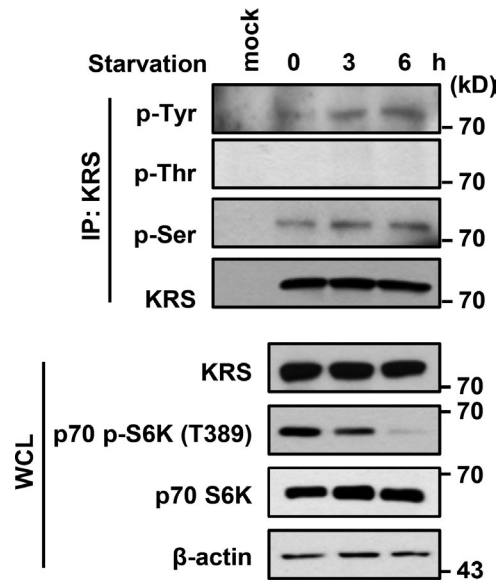
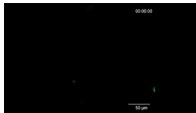
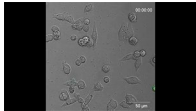


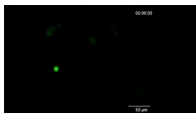
Figure S5. **The effect of starvation on the phosphorylation of KRS.** To see whether KRS is phosphorylated by starvation, KRS was immunoprecipitated (IP) with anti-KRS antibody from HCT116 cells starved for 0, 3, and 6 h, and the precipitated KRS was subjected to immunoblotting with anti-phospho-Ser, Tyr, and Thr antibodies. 100% of the immunoprecipitated samples were loaded for gel electrophoresis. WCL, whole-cell lysate.



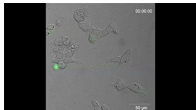
Video 1. **Complex formation between KRS-Venus-N and syntenin-Venus-C that restores green fluorescence was monitored by fluorescence microscopy in HCT116 cells incubated in normal conditions.** Frames were taken every 3 min for 3 h.



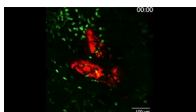
Video 2. **Green fluorescence generated by complex formation superimposed with cells observed by phase-contrast microscopy in normal conditions.** Merge of Video 1. Frames were taken every 3 min for 3 h.



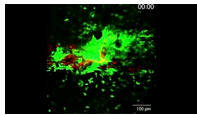
Video 3. **Complex formation between KRS-Venus-N and syntenin-Venus-C that restores green fluorescence was monitored by fluorescence microscopy in HCT116 cells incubated in starvation conditions.** Frames were taken every 3 min for 3 h.



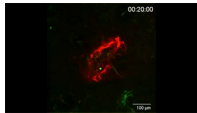
Video 4. **Green fluorescence generated by complex formation superimposed with cells observed by phase-contrast microscopy in starvation conditions.** Merge of Video 3. Frames were taken every 3 min for 3 h.



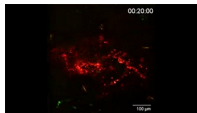
Video 5. **Time-lapse intravital microscopy showing the recruitment of macrophages/monocytes (green) to the injected BSA stained with Alexa Fluor 647 as described in the Intravital imaging section of Materials and methods.** BSA was injected into mouse ear dermis. After 6 h, frames were taken every 30 s for 30 min.



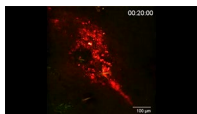
Video 6. Time-lapse intravital microscopy showing the recruitment of macrophages/monocytes (green) to the injected naked KRS stained with Alexa Fluor 647 as described in the Intravital imaging section of Materials and methods. Naked KRS was injected into mouse ear dermis. After 6 h, frames were taken every 30 s for 30 min.



Video 7. Time-lapse intravital microscopy shows the recruitment of macrophages/monocytes (green) to BSA stained with Alexa Fluor 647. Frames were taken every 30 s for 120 min.



Video 8. Time-lapse intravital microscopy shows the recruitment of macrophages/monocytes (green) to exosomes isolated from starved HCT116 cells that were treated with control siRNA stained with Dil (red fluorescence). Frames were taken every 30 s for 120 min.



Video 9. Time-lapse intravital microscopy shows the recruitment of macrophages/monocytes (green) to exosomes isolated from starved HCT116 cells that were treated with si-KRS stained with Dil (red fluorescence). Frames were taken every 30 s for 120 min.

## References

- Barchowsky, A., L.R. Klei, E.J. Dudek, H.M. Swartz, and P.E. James. 1999. Stimulation of reactive oxygen, but not reactive nitrogen species, in vascular endothelial cells exposed to low levels of arsenite. *Free Radic. Biol. Med.* 27:1405–1412. [http://dx.doi.org/10.1016/S0891-5849\(99\)00186-0](http://dx.doi.org/10.1016/S0891-5849(99)00186-0)
- Liang, C.C., A.Y. Park, and J.L. Guan. 2007. In vitro scratch assay: a convenient and inexpensive method for analysis of cell migration in vitro. *Nat. Protoc.* 2:329–333. <http://dx.doi.org/10.1038/nprot.2007.30>
- Piret, J.P., D. Mottet, M. Raes, and C. Michiels. 2002. CoCl<sub>2</sub>, a chemical inducer of hypoxia-inducible factor-1, and hypoxia reduce apoptotic cell death in hepatoma cell line HepG2. *Ann. N. Y. Acad. Sci.* 973:443–447. <http://dx.doi.org/10.1111/j.1749-6632.2002.tb04680.x>
- Ruiz-Ramos, R., L. Lopez-Carrillo, A.D. Rios-Perez, A. De Vizcaya-Ruiz, and M.E. Cebrian. 2009. Sodium arsenite induces ROS generation, DNA oxidative damage, HO-1 and c-Myc proteins, NF-κB activation and cell proliferation in human breast cancer MCF-7 cells. *Mutat. Res.* 674:109–115. <http://dx.doi.org/10.1016/j.mrgentox.2008.09.021>